International Journal of Nanomedicine

Dovepress
open access to scientific and medical research

Open Access Full Text Article

ORIGINAL RESEARCH

# Synergistic and complete reversal of the multidrug resistance of mitoxantrone hydrochloride by three-in-one multifunctional lipid-sodium glycocholate nanocarriers based on simultaneous BCRP and Bcl-2 inhibition



This article was published in the following Dove Press journal:
International Journal of Nanomedicine
23 August 2016
Number of times this article has been viewed

Guixia Ling[1]
Tianhong Zhang[2]
Peng Zhang[2]
Jin Sun[1]
Zhonggui He[1]

[1]Department of Pharmaceutics, [2]Department of Pharmaceutical Analysis, School of Pharmacy, Shenyang Pharmaceutical University, Shenyang, People's Republic of China

**Abstract:** Multidrug resistance (MDR) is a severe obstacle to successful chemotherapy due to its complicated nature that involves multiple mechanisms, such as drug efflux by transporters (P-glycoprotein and breast cancer resistance protein, BCRP) and anti-apoptotic defense (B-cell lymphoma, Bcl-2). To synergistically and completely reverse MDR by simultaneous inhibition of pump and non-pump cellular resistance, three-in-one multifunctional lipid-sodium glycocholate (GcNa) nanocarriers (TMLGNs) have been designed for controlled co-delivery of water-soluble cationic mitoxantrone hydrochloride (MTO), cyclosporine A (CsA – BCRP inhibitor), and GcNa (Bcl-2 inhibitor). GcNa and dextran sulfate were incorporated as anionic compounds to enhance the encapsulation efficiency of MTO (up to 97.8%±1.9%) and sustain the release of cationic MTO by electrostatic interaction. The results of a series of in vitro and in vivo investigations indicated that the TMLGNs were taken up by the resistant cancer cells by an endocytosis pathway that escaped the efflux induced by BCRP, and the simultaneous release of CsA with MTO further efficiently inhibited the efflux of the released MTO by BCRP; meanwhile GcNa induced the apoptosis process, and an associated synergistic antitumor activity and reversion of MDR were achieved because the reversal index was almost 1.0.

**Keywords:** mitoxantrone hydrochloride, three-in-one multifunctional lipid-GcNa nanocarriers, sodium glycocholate, multidrug resistance, breast cancer resistance protein, B-cell lymphoma

## Introduction

Multidrug resistance (MDR) is the most commonly encountered phenomenon that limits successful cancer chemotherapy.[1–3] Overcoming MDR has proved to be a great challenge due to the complicated mechanisms involved in MDR, including the overexpression of multidrug efflux transporters like P-glycoprotein and breast cancer resistance protein (BCRP),[4,5] and modifications in metabolism and changes in survival/apoptotic pathways like apoptosis-associated protein B-cell lymphoma (Bcl-2).[6] Despite its distinct mechanisms, MDR is usually the cumulative effect of a combination of MDR mechanisms such as blocked apoptosis and increased drug efflux.[7] Accordingly, there is an urgent need for the development of a simple, multifunctional, and effective vector that can concurrently and efficiently deliver a chemotherapeutic drug, an efflux pump inhibitor, and an anti-apoptotic defense suppressor into the cancer cells for complete and synergistic reversal of MDR.

Correspondence: Peng Zhang
Department of Pharmaceutical Analysis, School of Pharmacy, Shenyang Pharmaceutical University, 103 Wenhua Road, Shenyang 110016, People's Republic of China
Tel +86 24 2398 6291
Fax +86 24 2398 6250
Email zhangpengspu@163.com

submit your manuscript | www.dovepress.com
Dovepress
http://dx.doi.org/10.2147/IJN.S95767

Mitoxantrone hydrochloride (MTO, Figure S1A) is a synthetic anthracenedione chemotherapeutic drug that has been extensively used for the treatment of advanced breast and prostate cancers, lymphoma, and leukemia.[8–11] However, MTO is a substrate of efflux transporter BCRP, which results in severe MTO resistance in tumor cells.[12,13] To improve the efficacy of MTO chemotherapy, it is critical to establish new nanocarriers that can reduce the efflux, prolong the retention of MTO in drug-resistant cancer cells, overcome MDR, and reduce the side effects in normal tissues.

Nanostructured lipid carriers (NLCs), as potential anticancer drug delivery nanocarriers, exhibit great ability to modulate drug release, improve anticancer activity, and overcome MDR.[13] Although many lipophilic drugs can be easily encapsulated into NLCs,[14–16] it is a real challenge to design lipid-based nanocarriers for high encapsulation of water-soluble drugs (such as MTO) using conventional preparation processes.

In our previous study, nanostructured lipid–dextran sulfate hybrid carriers (NLDCs) were developed for controlled delivery of MTO in NLCs to overcome MDR.[17] The MTO-NLDCs increased the cytotoxicity and cellular accumulation, thereby overcoming the MDR of MTO. However, the resistant index (RI) of MTO-NLDCs was 9.8 and much higher than 1.0, which indicated that the MDR was only partly overcome.

Therefore, to completely reverse the MDR of MTO based on the simultaneous inhibition of pump and non-pump cellular resistance, in this study, we attempted to exploit three-in-one multifunctional lipid-sodium glycocholate (GcNa, Figure S1B) nanocarriers (TMLGNs) for efficient co-delivery of the cationic water-soluble anticancer drug, an efflux pump inhibitor, and Bcl-2 inhibitor into tumor cells. The combined chemotherapy system contains 1) TMLGNs as multifunctional co-delivery nanocarriers, 2) MTO as a cationic water-soluble anticancer drug, 3) cyclosporine A (CsA – BCRP inhibitor) that inhibits BCRP efflux as a suppressor of pump resistance, and 4) GcNa (Bcl-2 inhibitor) as a suppressor of non-pump cellular resistance.

CsA, as the best known BCRP inhibitor, can reduce the efflux of anticancer drugs and is commonly used as an MDR-reversing agent.[18,19] Therefore, to improve the efficacy of MTO, and efficiently reverse MDR, we encapsulated MTO and CsA simultaneously into TMLGNs for precise and controlled co-delivery into tumor cells.

Encapsulation of low-molecular-weight water-soluble ionic drugs, such as MTO, is a great challenge for NLCs using common preparation methods. In our previous study, we prepared NLDCs using dextran sulfate (DS, Figure S1C) as a negative ionic polymer to form an electrostatic complex with cationic MTO and increase the encapsulation efficiency of MTO.[17] In this study, we designed TMLGNs as an another type of prospective NLCs, in which a counterionic small molecule of GcNa (Bcl-2 inhibitor) was selected to complex with MTO by forming an ion pair and 1,2-Distearoyl-*sn*-glycero-3-phosphoethanolamine-*N*-[methoxy(polyethyleneglycol)-2000] (PEG-PE) was added to produce a prolonged circulation of TMLGNs. Most importantly, GcNa is a Bcl-2 inhibitor which can inhibit MDR and induce apoptosis.[20] GcNa plays dual important roles in TMLGNs: 1) as a suppressor of non-pump cellular resistance to promote tumor cell apoptosis and 2) as an anionic small molecule to increase the encapsulation efficiency and sustain the release of MTO in lipids by electrostatic interaction. GcNa has a similar amphiphilicity to the negatively charged hydrophilic and lipophilic part as DS. When the positive hydrophilic segment of MTO and the negative hydrophilic part of GcNa form a complex by electrostatic interaction, the lipophilicity of MTO would be improved and the charge neutralization would allow instantaneous entrapment of the complex into lipids.

A series of in vitro and in vivo characteristics of the prepared TMLGNs were systematically investigated using measurements of particle size, zeta potential, encapsulation efficiency, transmission electron microscopy imaging, differential scanning calorimetry (DSC), in vitro release, in vivo pharmacokinetics, and biodistribution. The cytotoxicity, synergistic reverse of MDR, and reversal mechanism of TMLGNs were further investigated to provide evidence that the "three-in-one" multifunctional nanosystem can completely overcome the MDR of MTO.

The present study was intended to provide evidence of a promising platform for combined chemotherapy by integrating the "BCRP bypassing effect" of TMLGNs, the "BCRP inhibition effect" of BCRP inhibitor, and the "apoptosis-inducing effect" of Bcl-2 inhibitor based on the advantages of nanocarriers and multiple mechanisms of MDR.

# Materials and methods

## Materials

Mitoxantrone dihydrochloride (99.4% purity) was provided by Beijing Xinze Tech. Co., Ltd. (Beijing, People's Republic of China). Compritol 888 ATO was kindly donated by Gattefosse (Weil am Rhein, Germany). Miglyol 812 was obtained from Caelo (D-Hilden, Germany). Cremophor RH40 and lecithin were purchased from BASF (Ludwigshafen, Germany). Dextran sulfate sodium (molecular weight 5,000 Da) was supplied by Shanghai Xibao Biotech. Co., Ltd (Shanghai, People's Republic of China). Other materials were supplied by Sigma-Aldrich (St Louis, MO, USA), while trypsin, RPMI 1640 medium, and fetal bovine serum were obtained from Gibco

BRL (Grand Island, NY, USA). 1,2-Distearoyl-*sn*-glycero-3-phosphoethanolamine-*N*-[methoxy(polyethyleneglycol)-2000] (PEG–PE) was obtained from Avanti Polar Lipids (Alabaster, AL, USA) and lecithin and GcNa were provided by BASF (Germany) and Sigma-Aldrich (USA), respectively. All solvents used in this study were of HPLC grade.

## Cell culture and animals

MCF-7 (human breast carcinoma cell line) and BCRP overexpressing MCF-7/MX (multidrug resistant variant) cells were provided by Nanjing Kaiji Biotech. Ltd. Co. (Nanjing, People's Republic of China). Cells were routinely cultured in RPMI-1640 medium supplemented with 10% fetal bovine serum at 37°C in a humidified atmosphere of 5% $CO_2$. Cells were regularly subcultured by trypsin/ethylenediaminetetraacetic acid upon reaching 80%–90% confluence. The cell experiments were carried out in compliance with the guidelines for the Care and Use of Cells of Shenyang Pharmaceutical University.

Twelve healthy adult male Wistar rats weighing 220±20 g and 20 male mice weighing 22–25 g (~12 weeks of age) (Laboratory Animal Center of Shenyang Pharmaceutical University, Shenyang, Liaoning, People's Republic of China) were housed in a room with controlled temperature and humidity and had free access to food and water. Before the day of administration via the tail vein, the animals were fasted for 12 hours but allowed water ad libitum. All the animal experiments were carried out in compliance with the guidelines for the Care and Use of Laboratory Animals of Shenyang Pharmaceutical University. Ethical approval was obtained for the use of animals in this study from the review board for the Care and Use of Cells/Laboratory Animals of Shenyang Pharmaceutical University.

## Preparation of MTO-TMLGNs

MTO-TMLGNs were prepared by the emulsification–ultrasonication method as previously described with some modifications.[17] In brief, Compritol 888 ATO, cremophor RH40, miglyol 812, lecithin, PEG–PE, and CsA (in a weight ratio of 4:2:1:1:3:0.125) were mixed and dissolved in ethanol by heating at 85°C. The ethanol was removed by magnetic stirring for 20 minutes and then MTO (with a weight ratio of 10% to the solid and liquid lipids) and GcNa-DS mixed aqueous solutions (weight ratio of 1:1.85) were added dropwise to the melted lipid under magnetic stirring. After 5 minutes of stirring, the obtained primary emulsion was diluted and ultrasonicated using a probe sonicator for 3 minutes at 300 W. The final nanoemulsion was cooled in an ice bath for 30 minutes to allow the formation of TMLGNs. After metering the volume by distilled water, the final concentration of MTO in the nanoparticle suspensions was 0.5 mg/mL. To confirm the effect of DS and GcNa in increasing the encapsulation efficiency, MTO-NLCs without DS and GcNa were prepared by the same procedure except that the GcNa-DS mixed solution was replaced by distilled water.

## Characterization of MTO-TMLGNs

MTO-TMLGNs were characterized by different investigations including the measurement of particle size, zeta potential, transmission electron microscope imaging, DSC, encapsulation efficiency, and in vitro release using similar procedures as in our previous study.[17] The transmission electron microscope images were obtained at 80 kV on a Hitachi (H-600) instrument (Tokyo, Japan). A Coulter LS 230 laser diffraction instrument and a zeta potential analyzer (Delsa 440SX) (Beckmann-Coulter Electronics, Krefeld, Germany) were used to measure the particle size and zeta potential of the nanoparticles, respectively. DSC analysis was conducted using a TA-60WS Thermal Analyzer (Shimadzu, Kyoto, Japan). The encapsulation efficiency and drug release of MTO were determined using a Sephadex G50 micro column centrifugation method and dialysis bag technique, respectively[17] (described in detail in the "Supplementary materials" section).

## Pharmacokinetics and tissue distribution study

For the pharmacokinetic study, 12 healthy adult male Wistar rats weighing 220±20 g (mean ± standard deviation [SD]) were randomly divided into two groups and MTO-Sol and MTO-TMLGNs were intravenously administered via the caudal vein at a single MTO dose of 1 mg/kg. Blood samples (250 μL) were collected into heparinized tubes by puncturing the retro-orbital sinus at determined times (0.08, 0.17, 0.33, 0.50, 1, 2, 4, 6, 8, 12, 24, and 48 hours of post-dosing). Plasma was obtained immediately by centrifugation at 2,000× *g* for 10 minutes and kept frozen at −80°C until analysis.

Twenty male mice weighing 22–25 g (~12 weeks of age) were randomized into groups according to their body weight for the tissue distribution investigation. MTO-Sol and MTO-TMLGNs were intravenously administered to the mice at a single dose of 1 mg/kg, and at 0.5 and 4 hours, blood samples were collected and plasma was separated. Heart, liver, spleen, lungs, kidneys, and brains were rapidly excised and homogenized following blood collection.

MTO concentrations in plasma and tissue homogenate were determined by LC-MS/MS after liquid–liquid extraction with diethyl ether–dichloromethane (3:2, v/v) with palmatine as the internal standard.[21]

## In vitro cytotoxicity assays

The cytotoxicity of MTO formulations (MTO-Sol, MTO-CsA-GcNa-Sol, and MTO-TMLGNs) was evaluated by MTT assay using MCF-7 and MCF-7/MX cells after incubation for 48, 72, and 96 hours.[17] The absorbance of the MTO formulations and control ($A_{\text{MTO formulations}}$ and $A_{\text{Control}}$) was measured by the microplate reader at wavelength of 570 nm. The sigmoidal dose–response curves for the inhibition rate versus the logarithm of the MTO concentration were constructed. The cell growth inhibition rate (%), 50% inhibition concentration ($IC_{50}$), resistant index (RI), and reversal factor (RF) were calculated to evaluate the cytotoxicity and MDR reversal effect.[17]

$$\text{Inhibition rate (\%)} = \left(1 - \frac{A_{\text{MTO formulations}}}{A_{\text{Control}}}\right) \times 100\% \quad (1)$$

$$\text{RI} = \frac{\text{IC}_{50\,(\text{MCF-7/MX})}}{\text{IC}_{50\,(\text{MCF-7})}} \quad (2)$$

$$\text{RF} = \frac{\text{IC}_{50\,(\text{MTO-Sol})}}{\text{IC}_{50\,(\text{MTO test formulations})}} \quad (3)$$

### Cellular uptake and its mechanism

The cell uptake efficiency of MTO in MCF-7 and MCF-7/MX cells was investigated after incubation with MTO formulations, including MTO-Sol, MTO-CsA-GcNa-Sol, and MTO-TMLGNs, at an MTO concentration of 100 nM for 2 hours at 37°C and 4°C.[17] The concentration of MTO in the cell supernatant was determined by a validated LC-MS/MS method with palmatine as the internal standard after extraction as described earlier.[21] The cell uptake efficiency was expressed as the percentage of determined MTO content in the incubated cells versus the total amount of MTO in the feed solution.

To further explore the possible mechanism of TMLGNs endocytosis via cancer cells, the uptake inhibition experiments were conducted in MCF-7/MX cells by treatment with 25 μM sodium azide, 50 μM chlorpromazine, and 100 μM indomethacin for 1 hour at 37°C prior to a 2 hour-incubation with MTO formulations.

## Statistical analysis

Student's *t*-test was performed to evaluate the significance of differences between the MTO-Sol and MTO-TMLGNs groups. Statistical significance was considered at $P<0.05$. All data were presented as mean ± SD (n=6 for the pharmacokinetic study and n=3 for the cellular uptake study).

# Results and discussion

## Characterization of TMLGNs

MTO is a synthetic antitumor drug composed of anthracenedione ring and positively charged groups (Figure S1A). The positively charged groups make MTO water soluble (logP=–3.1, pKa=8.13). It is very difficult to incorporate MTO into NLCs by applying conventional formulation processes because of the low drug partitioning in lipids. In our previous study, MTO-NLDCs were studied using negative ionic polymer DS to form an electrostatic complex with cationic MTO with increased encapsulation efficiency.[17] However, the MDR of MTO could be partly overcome by MTO-NLDCs. In the present study, we developed MTO-TMLGNs as another type of NLCs to completely reverse the MDR of MTO. GcNa was selected not only as a negative small molecule but also as a Bcl-2 inhibitor. The anionic GcNa was incorporated into TMLGNs as a counterionic small molecule to form an electrostatic complex with cationic MTO.

As illustrated in Figure 1, the TMLGNs were rationally designed as a solid–liquid mixed lipid core, a hydrophilic PEG shell, and an encapsulated CsA, MTO-DS, and MTO-GcNa electrostatic complex. Transmission electron microscope imaging (Figure 2A) was performed to characterize the morphology of TMLGNs. It was obvious that the TMLGNs were spherical in shape and did not adhere to each other. The diameter size distribution of TMLGNs is displayed in Figure 2B, from which narrow size distribution is shown. The mean diameter of TMLGNs was 125.0 nm with a polydispersity index of 0.21. The main physicochemical parameters of the prepared MTO-NLCs and MTO-TMLGNs are summarized in Table 1. The particle diameter of MTO-TMLGNs was not significantly different from that of MTO-NLCs, suggesting that the encapsulation of CsA, DS, and GcNa did not increase the particle size of the nanoparticles. The encapsulation efficiency of MTO in NLCs was only 36.5%, which is relatively low due to the low affinity of cationic MTO for hydrophobic lipids, while the encapsulation efficiency of MTO in TMLGNs was markedly increased to 97.8%, which indicated that GcNa and DS significantly increased the encapsulation efficiency of MTO in lipids. It has been reported that an electrostatic interaction between cationic drug and counterionic polymers or small molecules plays a prominent role in the development of nanocarriers.[17,22–29] MTO was incorporated into a mixed lipid core because of the strong electrostatic interaction between DS and GcNa. Moreover, a comparative analysis of the zeta potential of the blank NLCs

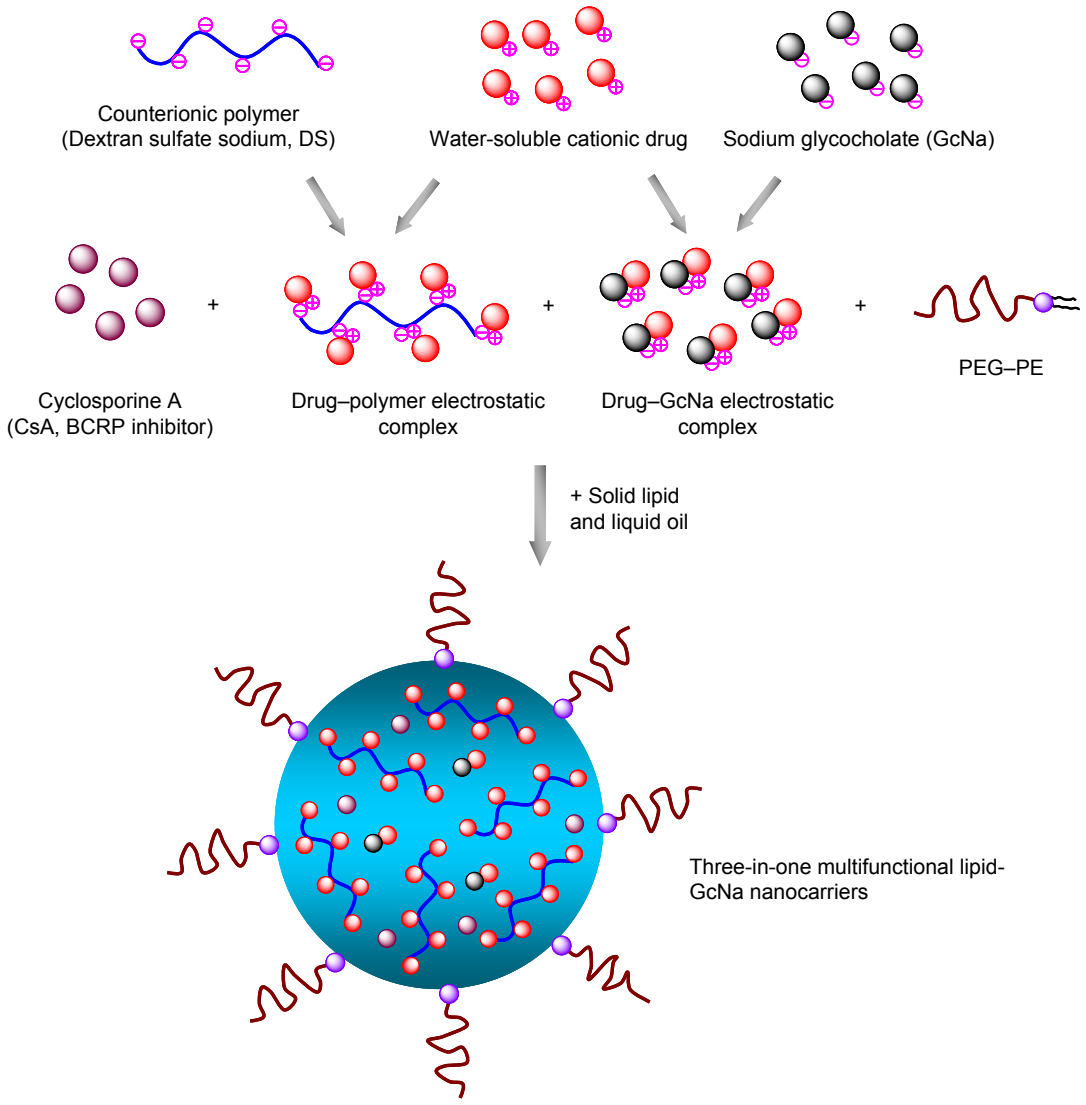


**Figure 1** The proposed schematic illustration of three-in-one multifunctional lipid-GcNa nanocarriers (TMLGNs).
**Abbreviations:** GcNa, sodium glycocholate; BCRP, breast cancer resistance protein; PEG-PE, 1,2-Distearoyl-*sn*-glycero-3-phosphoethanolamine-*N*-[methoxy (polyethyleneglycol)-2000].

(−31.3±2.5), MTO-NLCs (−19.9±1.4), and MTO-TMLGNs (−28.7±0.4) further confirmed the role of the electrostatic interaction between the MTO and GcNa/DS. It was reported that a zeta potential of at least −30 mV for electrostatically stabilized systems was necessary to obtain a physically stable formulation.[30] In this study, the zeta potential of the blank NLCs was −31.3±2.5 mV, which reflected the electrostatic repulsion and storage stability. Compared with the blank NLCs, the zeta potential of MTO-TMLGNs was not significantly changed owing to the neutralization of cationic MTO by anionic charges on the DS and GcNa, while that of MTO-NLCs was significantly increased because of the encapsulation of cationic MTO. Therefore, the electrostatic interaction between MTO and GcNa or MTO and DS made the MTO-TMLGNs negative as blank NLCs, and more negative than MTO-NLCs.

Formulation development of lipid nanoparticles aims physical stability in particle size and crystalline state of the lipid matrix.[31–33] Therefore, it is necessary to prove the solid state of the lipid in TMLGNs and investigate the influence of the incorporated drug on the melting behavior of lipid by DSC. DSC thermograms are shown in Figure 2C for pure MTO, CsA, GcNa raw material, blank excipients, physical mixture of drug and excipients, and lyophilized MTO-TMLGNs. The thermogram of the freeze-dried TMLGNs did not show any endothermic peak at 173.5°C that corresponds to the melting endothermic peak of MTO, which indicated that MTO was solubilized or dispersed in

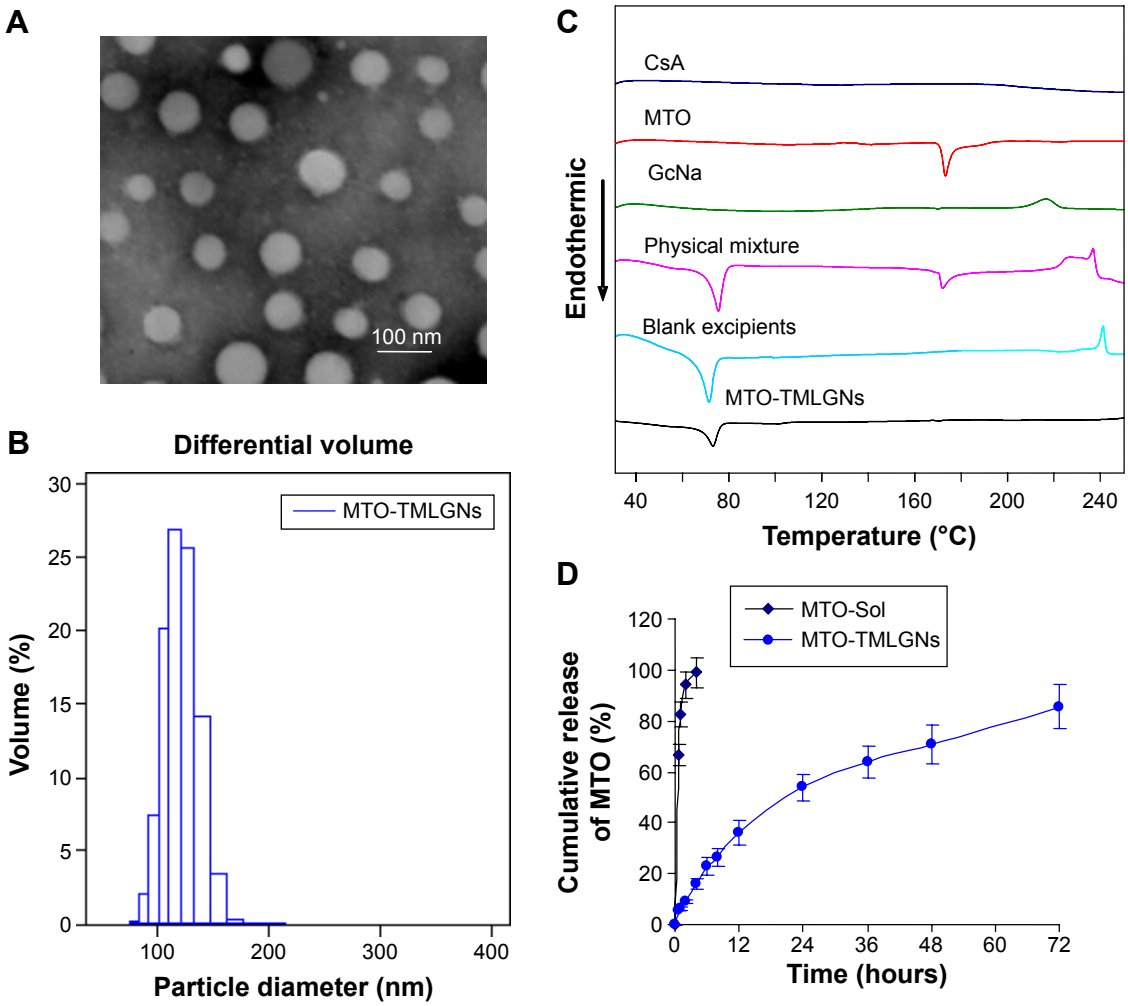


**Figure 2** Characterization of three-in-one multifunctional lipid-GcNa nanocarriers (TMLGNs).
**Notes:** (**A**) TEM. (**B**) Particle size distribution of TMLGNs. (**C**) DSC curves. (**D**) In vitro release profiles of MTO in pH 7.4 PBS containing 0.2% $Na_2SO_3$ from MTO-Sol, MTO-NLCs, and MTO-TMLGNs determined by the dialysis bag technique (mean ± SD, n=6).
**Abbreviations:** GcNa, sodium glycocholate; TEM, transmission electron microscopy; MTO, mitoxantrone hydrochloride; NLC, nanostructured lipid carrier; SD, standard deviation; DSC, differential scanning calorimetry; CsA, cyclosporine A; PBS, phosphate buffered saline.

the lipid phase during TMLGNs preparation. In contrast to the lipid in blank excipients, the phase transition of the TMLGNs was broader, which could be attributed to the presence of polydispersed nanoparticles. The results also showed that the incorporated drugs and other excipients did not significantly influence the melting temperature of the lipid: the values were between 72.5°C and 73.7°C in blank excipients, physical mixture, and lyophilized TMLGNs.

**Table 1** Summary of particle size, zeta potential, and drug encapsulation efficiency of MTO-NLCs and MTO-TMLGNs (mean ± SD, n=3)

| Nanoparticles | Particle size (nm) | Zeta potential (mV) | Encapsulation efficiency (%) |
|---|---|---|---|
| Blank NLCs | 130.4±4.6 | −31.3±2.5 | – |
| MTO-NLCs | 136.7±8.6 | −19.9±1.4** | 35.6±2.9 |
| MTO-TMLGNs | 125.0±4.0 | −28.7±0.4 | 97.8±1.9** |

**Notes:** Statistical significant difference compared to blank NLCs or MTO-NLCs; **$P<0.01$.
**Abbreviations:** MTO, mitoxantrone hydrochloride; NLC, nanostructured lipid carrier; SD, standard deviation; TMLGNs, three-in-one multifunctional lipid-GcNa nanocarriers; GcNa, sodium glycocholate.

## Release characteristics of TMLGNs

The introduction of GcNa and DS into TMLGNs not only increased the drug loading and encapsulation efficiency of MTO but also prolonged the release time up to 72 hours. The cumulative release of MTO from MTO-Sol and MTO-TMLGNs was determined by dialysis method and profiled as described in Figure 2D. It was investigated that 85.7% of MTO was released from the MTO-TMLGNs after 72 hours, while almost 100% was released from MTO-Sol after 4 hours. It was possible that ionic interaction and complexation between the MTO and carrageenan was so strong

that the MTO was released from the NLCCs as a complex. The property of gelatinization and the stability of carrageenan in neutral and alkaline conditions may have further sustained the release of MTO from the complex. This release style of drug as complex was similar to the previously reported data that found that doxorubicin was released from solid lipid nanoparticles as docosahexenoic acid (DHA)/doxorubicin lipophilic ion pairing/complex.[34]

Numerous methods for release determination are reported in the literature including dialysis-based methods,[35–37] ultracentrifugation,[38,39] centrifugal ultrafiltration,[40] and pressure ultrafiltration.[41,42] However, to our knowledge, no method is perfect for the release study to date. Release studies using dialysis misleadingly implied a slow release profile because the membrane transport effects masked the true release rate of drug from nanoparticles. Other ultrafiltration methods were validated the incomplete and inefficient separation of nanoparticles from the surrounding medium in which they were dispersed to produce a "clean" sample of unbound drug.[42]

## Pharmacokinetics and tissue distribution study

To achieve the effective delivery of cytotoxic agents with maximal antitumor efficacy and minimal side effects in normal tissues, suitable pharmacokinetic and biodistribution characteristics are indispensable. When water-soluble cytotoxic MTO was encapsulated into TMLGNs, great improvements were exhibited, such as sustained plasma profile, delayed retention in the systemic circulation, and moderate biodistribution.

The mean MTO plasma concentration–time curves in rats after the intravenous administration of MTO-Sol and MTO-TMLGNs at 1 mg/kg dose (n=6) are shown in Figure 3A and the pharmacokinetic parameters are listed in Table 2.

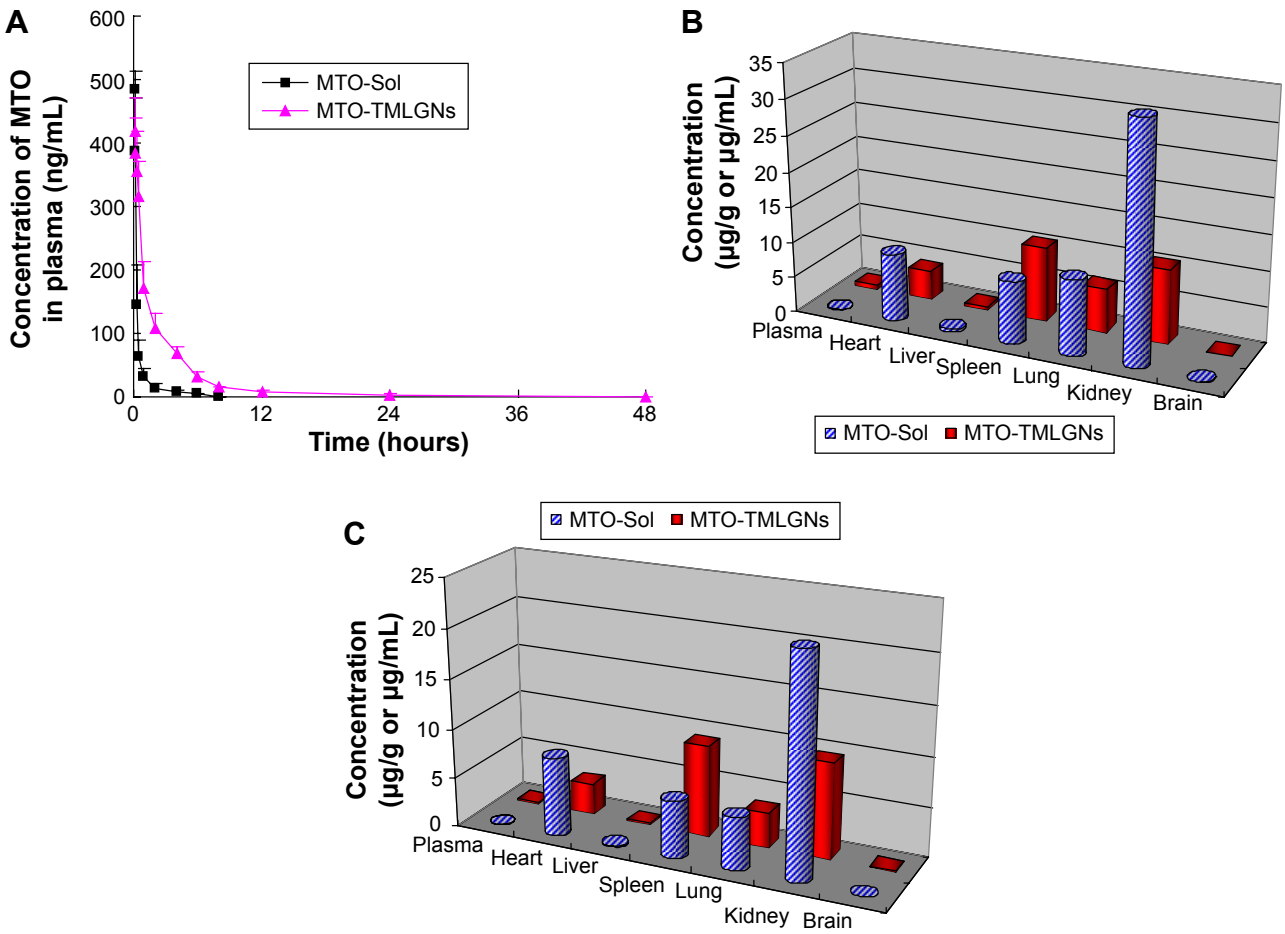


**Figure 3** Distribution of MTO in tissues of mice (**B** – 0.5 hour; **C** – 4 hours) and mean plasma concentration–time curves of MTO in rats after the intravenous administration of MTO-Sol and MTO-TMLGNs at a dose of 1 mg/kg (**A**) (mean ± SD, n=6).

**Abbreviations:** MTO, mitoxantrone hydrochloride; TMLGNs, three-in-one multifunctional lipid-GcNa nanocarriers; GcNa, sodium glycocholate; SD, standard deviation.

**Table 2** Main pharmacokinetic parameters of MTO in rats after the intravenous administration of MTO-Sol and MTO-TMLGNs at dose 1 mg/kg (mean ± SD, n=6)

| Parameters | MTO-Sol | MTO-TMLGNs |
|---|---|---|
| $C_{max}$ (ng/mL) | 485.0±27.6 | 419.1±52.6** |
| $t_{1/2}$ (h) | 1.52±0.18 | 10.72±0.89** |
| $AUC_{0-t}$ (ng/mL·h) | 201.9±58.3 | 928.0±172.6** |
| $AUC_{0-\infty}$ (ng/mL·h) | 203.5±58.3 | 943.7±174.8** |

**Notes:** **Statistical significant difference between MTO-Sol and MTO-TMLGNs group; $P<0.01$.

**Abbreviations:** MTO, mitoxantrone hydrochloride; TMLGNs, three-in-one multifunctional lipid-GcNa nanocarriers; GcNa, sodium glycocholate; SD, standard deviation.

Significant differences ($P<0.01$) were found for the pharmacokinetic parameters $C_{max}$, $t_{1/2}$, $AUC_{0-t}$, and $AUC_{0-\infty}$ between the two groups after the intravenous administration of MTO-Sol and MTO-TMLGNs (Table 2). Compared with the MTO-Sol group, the $AUC_{0-\infty}$ and $t_{1/2}$ of the MTO-TMLGNs group increased approximately 4.6-fold and 7.0-fold, respectively, which indicated that MTO-TMLGNs had a higher drug systematic exposure ($AUC_{0-t}$) than MTO-Sol, and the drug circulation time ($t_{1/2}$) was significantly prolonged by MTO-TMLGNs.

The results of the tissue distribution study are shown in Figure 3B and C. MTO-TMLGNs had a higher MTO concentration in plasma, spleen, and brain, but reduced distribution of MTO in heart, kidney, and lung. The biodistribution characteristics of MTO were significantly changed by MTO-TMLGNs.

Compared with MTO-Sol, MTO-TMLGNs reduced the MTO exposure to heart tissue approximately 0.6-fold, which is of great importance for reducing the toxicity of MTO, since the clinical use of MTO is limited by unwanted side effects, particularly dose-related cardiomyopathy.[43–46]

## In vitro cytotoxicity

The cytotoxicity of MTO-Sol, MTO-CsA-GcNa-Sol, and MTO-TMLGNs was investigated and compared in MCF-7 and MCF-7/MX cells. The dose–response curves are shown in Figure 4A–D and the calculated $IC_{50}$ values are given in Figure 4E.

As shown in Figure 4A–D, the growth inhibition effect of MTO-TMLGNs in MCF-7 cells was stronger than that of MTO-Sol, which indicated that using TMLGNs as nanocarriers increased the delivery efficiency of MTO into cancer cells. After incubation for 48, 72, and 96 hours with MCF-7/MX cells, the cytotoxicity of MTO in three different preparation groups was time-dependent; however, the magnitude of this effect was different.

In Figure 4E, the $IC_{50}$ of the five different groups were compared at the same time, and the $IC_{50}$ values were in the order of MTO-Sol>MTO-CsA-GcNa-Sol>MTO-TMLGNs. The cytotoxicity of MTO-TMLGNs was the greatest, which indicated that the TMLGNs significantly increased the sensitivity of MTO to resistant tumor cells. It was proved that the multicomponents co-encapsulated in the nanosystems were the most efficient dosage regimen for antitumor treatment because it takes advantage of nanocarriers in cancer therapy and combines multicomponents to obtain synergistic antitumor efficacy. While the cytotoxicity of the two solutions was weaker, and that of MTO-Sol was the weakest, MTO-VRP-GcNa-Sol was the next that was due to the cell apoptosis–promoting effect of GcNa.

The RI and RF were calculated to quantitatively assess the reversal effect on MDR by TMLGNs. In Table 3, the RI value of MTO-Sol was 55.0, which suggested that the sensitivity of cytotoxicity against resistant MCF-7/MX cells was significantly reduced, and the MCF-7/MX cells with a strong MTO-resistant effect are regarded as good model cells for the study of MDR. The RI values of MTO-TMLGNs, MTO-NLDCs, and MTO-CsA-GcNa-Sol were markedly reduced to 1.1, 9.8, and 7.0 (97.8%, 82.2%, and 87.2% reduction) compared with that of MTO-Sol, respectively. This suggested that when MTO was encapsulated into TMLGNs, the sensitivity to resistant cells was increased similar to sensitive cancer cells because the RI value was close to 1, and the MDR effect was completely reversed, while that of MTO-NLDCs was only partially overcome.

Table 3 shows the RFs of different formulations of MTO compared with MTO-Sol in MCF-7/MX cells at 48, 72, and 96 hours. The sequential order of RF was MTO-NLDCs[17]<MTO-CsA-GcNa-Sol<<MTO-TMLGNs. With MTO-Sol as a reference, the calculated RF values of MTO-TMLGNs in MCF-7/MX cells at 48, 72, and 96 hours were 226.8, 265.6, and 389.6, respectively. This demonstrated that the reversal effect MTO-TMLGNs on MDR was increased over time, while the change in MTO-CsA-GcNa-Sol was not obvious and was reduced at 48 and 96 hours. The RF value of MTO-TMLGNs was significantly higher than that of the other formulations and was 28.4-fold and 34.8-fold that of MTO-CsA-GcNa-Sol and MTO-NLDCs, respectively. This indicated that the reversal effect of MTO-TMLGNs on MDR was the strongest. The MDR of MTO was completely overcome by TMLGNs (RI was almost 1.0) because a synergistic MDR reversal effect was obtained by the co-encapsulation of MTO, BCRP, and Bcl-2 inhibitor into TMLGNs.

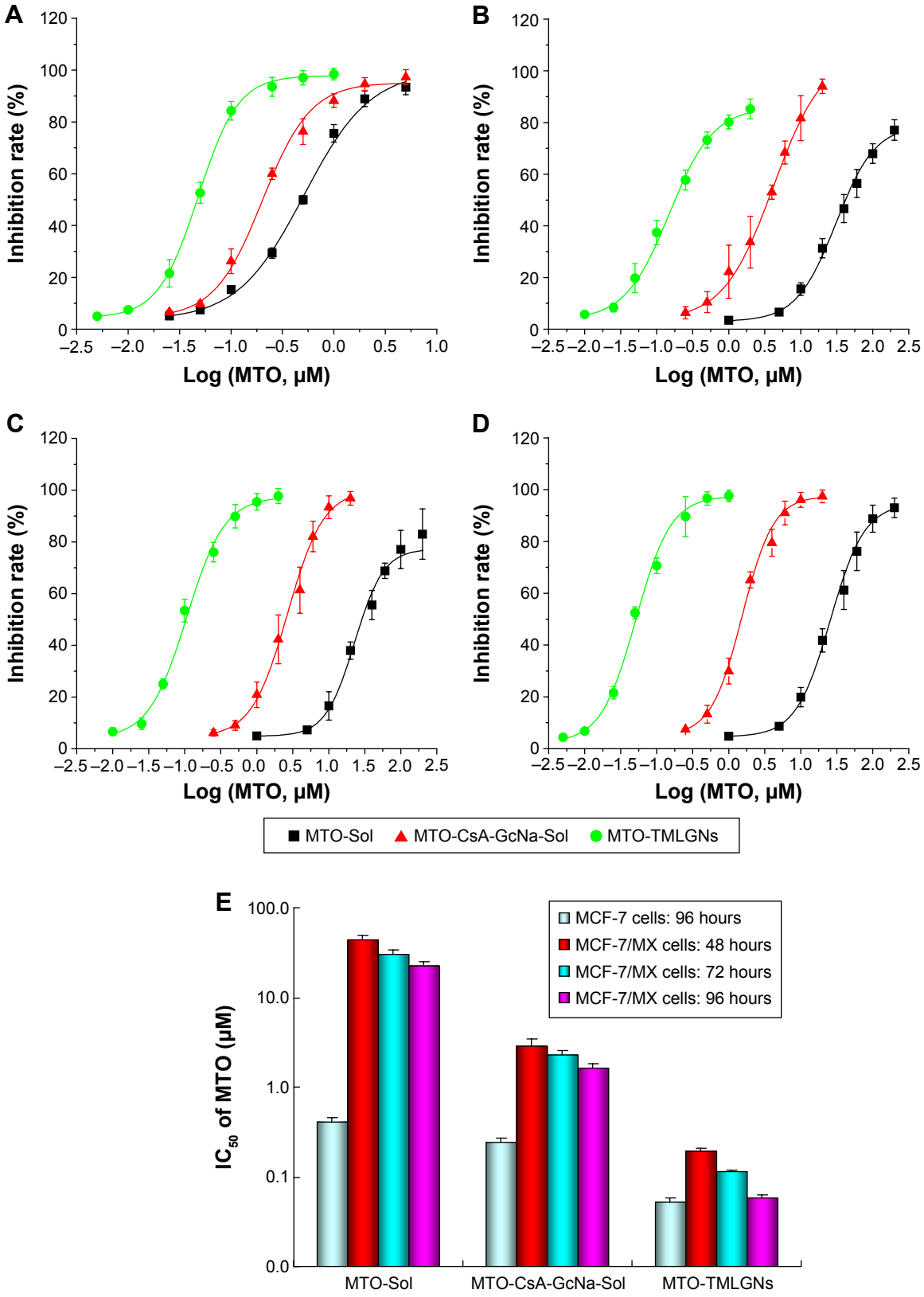


**Figure 4** In vitro cytotoxicity of MTO-Sol, MTO-CsA-GcNa-Sol, and MTO-TMLGNs.

**Notes:** Dose–response curves of MTO in MTO-Sol, MTO-CsA-GcNa-Sol, and MTO-TMLGNs. Curves of (**A**) MCF-7 cells for 96 hours; (**B**) MCF-7/MX cells for 48 hours; (**C**) MCF-7/MX cells for 72 hours; and (**D**) MCF-7/MX cells for 96 hours. (**E**) The 50% inhibition concentration ($IC_{50}$) of MTO-Sol, MTO-CsA-GcNa-Sol and MTO-TMLGNs against MCF-7/MX cells for 48, 72, and 96 hours and MCF-7 cells for 96 hours (mean ± SD, n=3).

**Abbreviations:** MTO, mitoxantrone hydrochloride; TMLGNs, three-in-one multifunctional lipid-GcNa nanocarriers; GcNa, sodium glycocholate; CsA, cyclosporine A; SD, standard deviation.

**Table 3** The reversal factor (RF) of MTO formulations compared to MTO-Sol in MCF-7/MX cells at 48, 72, and 96 hours, and the resistant index (RI) of MTO formulations in MCF-7/MX compared to MCF-7 cells at 96 hours

| MTO formulations | RI | RF | | |
|---|---|---|---|---|
| | 96 hours | 48 hours | 72 hours | 96 hours |
| MTO-Sol | 55.0 | – | – | – |
| MTO-CsA-GcNa-Sol | 7.0 | 15.1 | 13.0 | 13.7 |
| MTO-TMLGNs | 1.1 | 226.8 | 265.6 | 389.6 |
| MTO-NLDCs[17] | 9.8 | 7.8 | 10.1 | 11.2 |

**Abbreviations:** MTO, mitoxantrone hydrochloride; TMLGNs, three-in-one multifunctional lipid-GcNa nanocarriers; GcNa, sodium glycocholate; CsA, cyclosporine A; NLDCs, nanostructured lipid–dextran sulfate hybrid carriers.

The MDR of MTO was difficult to overcome due to the complicated mechanisms involved, such as drug efflux induced by BCRP and cell apoptosis inhibition by Bcl-2. In our previous studies, we developed NLDCs for the delivery of MTO which could partly reverse the MDR of MTO by inhibition of BCRP efflux[17] because the RI of MTO multifunctional nanoassemblies (MTO-MNAs) was 4.3, which was greater than 1. It is supposed that when MTO-MNAs are taken up into resistant cancer cells by endocytosis, a portion of MTO would be released, and then undergo efflux by BCRP transporter. So, if the BCRP inhibitor can be co-encapsulated into one nanocarrier and simultaneously delivered to cancer cells, the reversal effect on MDR will be further enhanced and the problem of the low efficiency and high toxicity of the BCRP inhibitor would be effectively overcome. Based on these findings, the MTO-TMLGNs as a three-in-one system were developed for the co-delivery of MTO, CsA, and GcNa in the present study. It had been validated that the developed MTO-TMLGNs significantly increased the cytotoxicity of MTO in the BCRP overexpressing MCF-7/MX cells and completely reversing the MDR of MTO (shown as an RI value close to 1).

## Effect of TMLGNs on cellular uptake of MTO

To investigate whether increased cytotoxicity of MTO-TMLGNs was helped by the increased accumulation, the cellular uptake of MTO in different formulations was compared in BCRP-overexpressing MCF-7/MX cells. As shown in Figure 5A, MTO-TMLGNs accumulated in MCF-7/MX cells to a greater extent than MTO-Sol alone, and the uptake efficiency of MTO-TMLGNs in MCF-7/MX cells was 12.8-fold higher than that of MTO-Sol, implying that BCRP-mediated drug efflux was markedly reduced by the introduction of TMLGNs.

## Uptake mechanisms of MTO-TMLGNs

The endocytosis of nanomedicines into cells has been reported to involve several pathways, including lipid raft/caveolae- and clathrin-mediated pathways, as well as macropinocytosis.[47,48] To elucidate the underlying MDR reversal mechanisms, the uptake mechanism of MTO-TMLGNs was investigated through temperature and endocytosis inhibition experiments in resistant MCF-7/MX cells. In addition, the different dosage regimens were compared to investigate the synergic MDR reversal effect of CsA and GcNa. The results (Figure 5B) demonstrated that the cellular uptake efficiency of MTO was clearly reduced at 4°C. Compared with the control group without inhibitor, the cellular uptake efficiency of MTO was found to be significantly inhibited by sodium azide (an energy inhibitor) and chlorpromazine (a clathrin-mediated endocytosis inhibitor) but not by indomethacin (a caveolae-mediated endocytosis inhibitor) ($P<0.01$, Figure 5B), which indicated that the uptake of MTO-TMLGNs might be energy-dependent endocytosis processes involving clathrin-mediated but not caveolae-mediated pathways. Clathrin-mediated endocytosis is a classical internalization pathway for macromolecules.[47–50] Extracellular substances are incorporated into clathrin-coated pits, which pinch off from plasma membrane, and are then internalized by the cell along with these pits.

In summary, the mechanism for the complete reversal of MDR by TMLGNs can be assumed to be that shown in Figure 5C: 1) the MTO-TMLGNs were taken up into BCRP-overexpressing MCF-7/MX cells by endocytosis, which increased the MTO accumulation in resistant cancer cells by escaping the efflux induced by BCRP transporter; 2) the released CsA further inhibited the efflux of the simultaneously released MTO; 3) GcNa inhibited Bcl-2 and promoted cancer cell apoptosis; and 4) the TMLGNs increased the delivery efficiency of the multicomponents and allowed them to act synergistically. The TMLGNs developed in this study will offer information to help develop an optimum regimen for water-soluble cytotoxic drugs in cancer treatment to completely reverse MDR.

# Conclusion

TMLGNs were developed for the synergistic and complete reversal of the MDR of MTO based on simultaneous BCRP and Bcl-2 inhibition. GcNa was selected as a dual-functional molecule to prepare TMLGNs, which not only increased the encapsulation efficiency by forming an electrostatic complex with cationic water-soluble drug MTO but also promoted cell

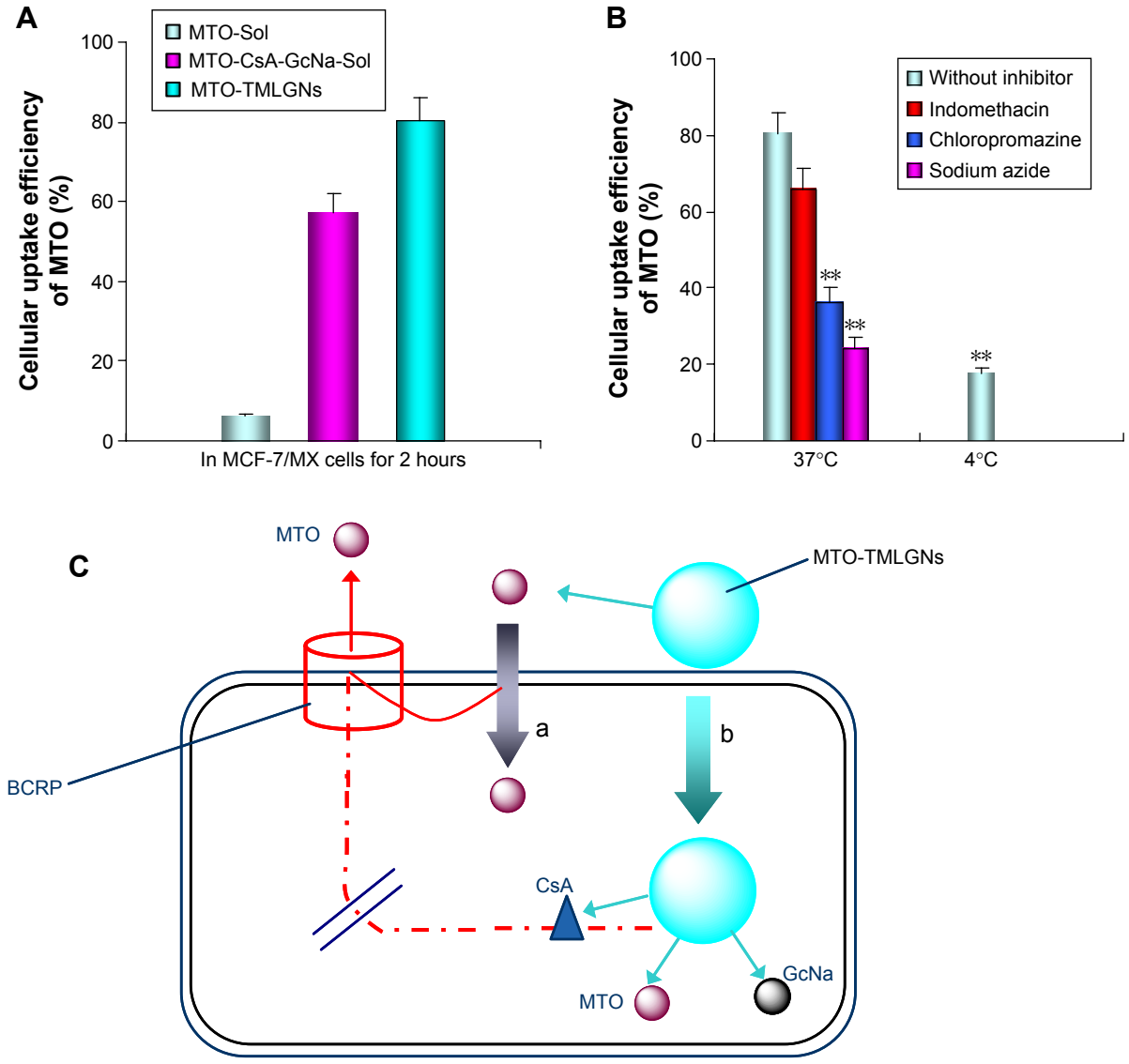


**Figure 5** Cell uptake and endocytosis mechanism of MTO-TMLGNs.

**Notes:** (**A**) Cell uptake efficiency of MTO in MCF-7/MX cells after incubation with MTO-Sol, MTO-CsA-GcNa-Sol, and MTO-TMLGNs at an MTO concentration of 100 nM for 2 hours. (**B**) Effects of incubation temperature and endocytosis inhibitors on the uptake efficiency of MTO in MCF-7/MX cells after incubation with MTO-TMLGNs at an MTO concentration of 100 nM for 2 hours. (**C**) Schematic illustration of the proposed mechanism indicating the increased anticancer activity and reversed multidrug resistance by MTO-TMLGNs – (a) diffusion of released free MTO across the cell membrane and (b) endocytosis of MTO-TMLGNs. **Statistical significant difference compared to uptake efficiency of MTO without inhibitor, $P<0.01$.

**Abbreviations:** MTO, mitoxantrone hydrochloride; TMLGNs, three-in-one multifunctional lipid-GcNa nanocarriers; GcNa, sodium glycocholate; CsA, cyclosporine A.

apoptosis by inhibiting Bcl-2. The multifunctional nanocarrier TMLGNs were very effective for the delivery of cationic hydrophilic drugs with sustained-release characteristics, an excellent pharmacokinetic profile, and they improved cellular uptake and cytotoxicity in resistant cancer cells. In particular, TMLGNs were capable of entering into cancer cells by clathrin-mediated endocytosis, which bypassed the efflux mediated by BCRP transporter, and simultaneously released CsA which further inhibited the released MTO, thereby completely overcoming the MDR of MTO by the synergistic effect of GcNa. Therefore, the co-encapsulation of a hydrophilic antitumor drug, BCRP inhibitor, and Bcl-2 inhibitor into TMLGNs is an optimum platform for the complete reversal of MDR.

## Acknowledgment

We are grateful for the financial support from the National Natural Science Foundation of China (81202480, 81302723) and the Natural Science Foundation of Liaoning Province (ZCJJ2014410/2015020749).

## Disclosure

The authors report no conflicts of interest in this work.

## References


1. Iyer AK, Singh A, Ganta S, Amiji MM. Role of integrated cancer nanomedicine in overcoming drug resistance. *Adv Drug Deliv Rev*. 2013;65:1784–1802.
2. Donnenberg VS, Donnenberg AD. Multiple drug resistance in cancer revisited: the cancer stem cell hypothesis. *J Clin Pharmacol*. 2005;45:872–877.
3. Stein WD, Bates SE, Fojo T. Intractable cancers: the many faces of multidrug resistance and the many targets it presents for therapeutic attack. *Curr Drug Targets*. 2004;5:333–346.
4. Duhem C, Ries F, Dicato M. What does multidrug resistance (MDR) expression mean in the clinic? *Oncologist*. 1996;1:151–158.
5. Dean M, Allikmets R. Complete characterization of the human ABC gene family. *J Bioenerg Biomembr*. 2001;33:475–479.
6. Kirkin V, Joos S, Zörnig M. The role of Bcl-2 family members in tumorigenesis. *Biochim Biophys Acta*. 2004;1644:229–249.
7. Gottesman MM, Fojo T, Bates SE. Multidrug resistance in cancer: role of ATP-dependent transporters. *Nat Rev Cancer*. 2002;2:48–58.
8. Khalaf A, Pfister C, Hellot MF, Dunet F, Moussu J, Grise P. Value of mitoxantrone in metastatic hormone-resistant prostate cancer. *Prog Urol*. 2002;12:37–42.
9. Hagemeister F, Cabanillas F, Coleman M, Gregory SA, Zinzani PL. The role of mitoxantrone in the treatment of indolent lymphomas. *Oncologist*. 2005;10:150–159.
10. Novoselac AV, Reddy S, Sanmugarajah J. Acute promyelocytic leukemia in a patient with multiple sclerosis following treatment with mitoxantrone. *Leukemia*. 2004;18:1561–1562.
11. Doyle LA, Yang W, Abruzzo LV, et al. A multidrug resistance transporter from human MCF-7 breast cancer cells. *Proc Natl Acad Sci U S A*. 1998;95:15665–15670.
12. Maliepaard M, van Gastelen MA, de Jong LA, et al. Overexpression of the BCRP/MXR/ABCP gene in a topotecan-selected ovarian tumor cell line. *Cancer Res*. 1999;59:4559–4563.
13. Kang KW, Chun MK, Kim O, et al. Doxorubicin-loaded solid lipid nanoparticles to overcome multidrug resistance in cancer therapy. *Nanomedicine*. 2010;6:210–213.
14. Müller RH, Radtke M, Wissing SA. Nanostructured lipid matrices for improved microencapsulation of drugs. *Int J Pharm*. 2002;242:121–128.
15. Ricci M, Puglia C, Bonina F, Di Giovanni C, Giovagnoli S, Rossi C. Evaluation of indomethacin percutaneous absorption from nanostructured lipid carriers (NLC): in vitro and in vivo studies. *J Pharm Sci*. 2005;94:1149–1159.
16. Yuan H, Wang LL, Du YZ, You J, Hu FQ, Zeng S. Preparation and characteristics of nanostructured lipid carriers for control-releasing progesterone by melt-emulsification. *Colloids Surf B Biointerfaces*. 2007;60:174–179.
17. Zhang P, Ling G, Pan X, et al. Novel nanostructured lipid-dextran sulfate hybrid carriers (NLDCs) overcome tumor multidrug resistance of mitoxantrone hydrochloride. *Nanomedicine*. 2012;8(2):185–193.
18. Kathawala RJ, Gupta P, Ashby CR Jr, Chen Z-S. The modulation of ABC transporter-mediated multidrug resistance in cancer: a review of the past decade. *Drug Resist Updat*. 2015;18:1–17.
19. Li L, Yao QQ, Xu SY, et al. Cyclosporin A affects the bioavailability of ginkgolic acids via inhibition of P-gp and BCRP. *Eur J Pharm Biopharm*. 2014;88(3):759–767.
20. Lo YL, Ho CT, Tsai FL. Inhibit multidrug resistance and induce apoptosis by using glycocholic acid and epirubicin. *Eur J Pharm Sci*. 2008;35:52–67.
21. Zhang P, Ling GX, Sun J, et al. Determination of mitoxantrone in rat plasma by liquid chromatography-tandem mass spectrometry method: application to a pharmacokinetic study. *J Chromatogr B Analyt Technol Biomed Life Sci*. 2010;878:2260–2265.
22. Song X, Cai Z, Zheng Y, et al. Reversion of multidrug resistance by co-encapsulation of vincristine and verapamil in PLGA nanoparticles. *Eur J Pharm Sci*. 2009;37:300–305.
23. Wang Y, Lu X, Lu W, Zhang C, Liang W. Pegylated phospholipids-based self-assembly with water-soluble drugs. *Pharm Res*. 2010;27:361–370.
24. Li Y, Taulier N, Rauth AM, Wu X. Screening of lipid carriers and characterization of drug-polymer-lipid interactions for the rational design of polymer-lipid hybrid nanoparticles (PLN). *Pharm Res*. 2006;23:1877–1887.
25. Ling G, Zhang P, Zhang W, et al. Development of novel self-assembled DS-PLGA hybrid nanoparticles for improving oral bioavailability of vincristine sulfate by P-gp inhibition. *J Control Release*. 2010;148:241–248.
26. Zhang P, Ling G, Sun J, et al. Multifunctional nanoassemblies for vincristine sulfate delivery to overcome multidrug resistance by escaping P-glycoprotein mediated efflux. *Biomaterials*. 2011;32(23):5524–5533.
27. Li YQ, Wong HL, Shuhendler AJ, Rauth AM, Wu XY. Molecular interactions, internal structure and drug release kinetics of rationally developed polymer–lipid hybrid nanoparticles. *J Control Release*. 2008;128:60–70.
28. Wong HL, Rauth AM, Bendayan R, et al. A new polymer–lipid hybrid nanoparticle system increases cytotoxicity of doxorubicin against multidrug-resistant human breast cancer cells. *Pharm Res*. 2006;23:1574–1585.
29. Wong HL, Bendayan R, Rauth AM, Wu XY. Simultaneous delivery of doxorubicin and GG918 (Elacridar) by new polymer–lipid hybrid nanoparticles (PLN) for enhanced treatment of multidrug-resistant breast cancer. *J Control Release*. 2006;116:275–284.
30. Jacobs C, Kayser O, Müller RH. Nanosuspensions as a new approach for the formulation for the poorly soluble drug tarazepide. *Int J Pharm*. 2000;196(2):161–164.
31. Shah R, Eldridge D, Palombo E, Harding I. Characterization. *Lipid Nanoparticles: Production, Characterization and Stability*. Springer-Briefs in Pharmaceutical Science & Drug Development; 2015;45–74.
32. Shah RM, Malherbe F, Eldridge D, Palombo EA, Harding IH. Physicochemical characterization of solid lipid nanoparticles (SLNs) prepared by a novel microemulsion technique. *J Colloid Interface Sci*. 2014;428:286–294.
33. Kovačevića AB, Müllerb RH, Savića SD, Vuletaa GM, Keck CM. Solid lipid nanoparticles (SLN) stabilized with polyhydroxy surfactants: preparation, characterization and physical stability investigation. *Colloids Surfaces A: Physicochem Eng Aspects*. 2014;444:15–25.
34. Mussi SV, Silva RC, Oliveira MC, Lucci CM, Azevedo RB, Ferreira LA. New approach to improve encapsulation and antitumor activity of doxorubicin loaded in solid lipid nanoparticles. *Eur J Pharm Sci*. 2013;48(1–2):282–290.
35. Sezer AD, Akbuga J, Bas AL. In vitro evaluation of enrofloxacinloaded MLV liposomes. *Drug Deliv*. 2007;14:47–53.
36. Muthu MS, Singh S. Poly (D, L-lactide) nanosuspensions of risperidone for parenteral delivery: formulation and in-vitro evaluation. *Curr Drug Deliv*. 2009;6:62–68.
37. D'Souza SS, DeLuca PP. Methods to assess in vitro drug release from injectable polymeric particulate systems. *Pharm Res*. 2006;23:460–474.
38. Martins S, Tho I, Reimold I, et al. Brain delivery of camptothecin by means of solid lipid nanoparticles: formulation design, in vitro and in vivo studies. *Int J Pharm*. 2012;439(1–2):49–62.
39. Sun J, Bi C, Chan HM, Sun S, Zhang Q, Zheng Y. Curcumin-loaded solid lipid nanoparticles have prolonged in vitro antitumour activity, cellular uptake and improved in vivo bioavailability. *Colloids Surf B Biointerfaces*. 2013;111:367–375.
40. Wang D, Kong L, Wang J, He X, Li X, Xiao Y. Polymyxin E sulfate-loaded liposome for intravenous use: preparation, lyophilization, and toxicity assessment in vivo. *PDA J Pharm Sci Technol*. 2009;63:159–167.

41. Boyd BJ. Characterisation of drug release from cubosomes using the pressure ultrafiltration method. *Int J Pharm*. 2003;260(2):239–247.
42. Wallace SJ, Li J, Nation RL, Boyd BJ. Drug release from nanomedicines: selection of appropriate encapsulation and release methodology. *Drug Deliv Transl Res*. 2012;2(4):284–292.
43. Faulds D, Balfour JA, Chrisp P, Langtry HD. Mitoxantrone. A review of its pharmacodynamic and pharmacokinetic properties, and therapeutic potential in the chemotherapy of cancer. *Drugs*. 1991;41:400–449.
44. Keefe DL. Anthracycline-induced cardiomyopathy. *Semin Oncol*. 2001; 28:2–7.
45. Jain KK. Evaluation of mitoxantrone for the treatment of multiple sclerosis. *Expert Opin Investig Drugs*. 2000;9:1139–1149.
46. Rentsch KM, Horber DH, Schwendener RA, Wunderli-Allenspach H, Hänseler E. Comparative pharmacokinetic and cytotoxic analysis of three different formulations of mitoxantrone in mice. *Br J Cancer*. 1997; 75:986–992.
47. Sahay G, Alakhova DY, Kabanov AV. Endocytosis of nanomedicines. *J Controlled Release*. 2010;145(3):182–195.
48. Chai GH, Hu FQ, Sun J, Du YZ, You J, Yuan H. Transport pathways of solid lipid nanoparticles across Madin-Darby canine kidney epithelial cell monolayer. *Mol Pharm*. 2014;11(10):3716–3726.
49. Martins S, Costa-Lima S, Carneiro T, Cordeiro-da-Silva A, Souto EB, Ferreira DC. Solid lipid nanoparticles as intracellular drug transporters: an investigation of the uptake mechanism and pathway. *Int J Pharm*. 2012; 430(1–2):216–227.
50. McMahon HT, Boucrot E. Molecular mechanism and physiological functions of clathrin-mediated endocytosis. *Nat Rev Mol Cell Biol*. 2011;12(8):517−533.

# Supplementary materials

## Characterization of MTO-TMLGNs

The mitoxantrone hydrochloride and three-in-one multifunctional lipid-sodium glycocholate (GcNa) nanocarriers (MTO-TMLGNs) were characterized by different investigations including particle size, zeta potential, transmission electron microscopy (TEM), differential scanning calorimetry (DSC), encapsulation efficiency, and in vitro release using the procedures similar to those described in our previous study.[1]

### Particle size and zeta potential

The particle size of the prepared nanoparticles was determined using a Coulter LS 230 laser diffraction instrument (Beckmann-Coulter Electronics, Krefeld, Germany). The nanoparticle suspensions were diluted 30-fold with water for injection to give an intensity of 300 Im as recommended by the manufacturer. The zeta potential was measured by a zeta potential analyzer (Delsa 440SX; Beckmann-Coulter Electronics) with the nanoparticles diluted in water. All the analyses were carried out in triplicate.

### Drug encapsulation efficiency

The encapsulation efficiency of MTO in nanoparticles was determined using Sephadex® G-50 micro column centrifugation method (Pfizer, New York, NY, USA). To separate the loaded MTO in nanoparticles and free MTO, 0.5 mL nanoparticle suspensions with MTO concentration of 0.5 mg/mL was loaded into the Sephadex micro column and eluted by 1 mL 0.001 M HCl for several times through centrifugation at 100× *g*. The eluted fractions containing MTO-loaded nanoparticles and free MTO were collected respectively for the determination of MTO by ultraviolet (UV) spectrophotometer at 610 nm.

For the determination of loaded MTO in nanoparticles, 1 mL nanoparticle suspension and suitable quantity of

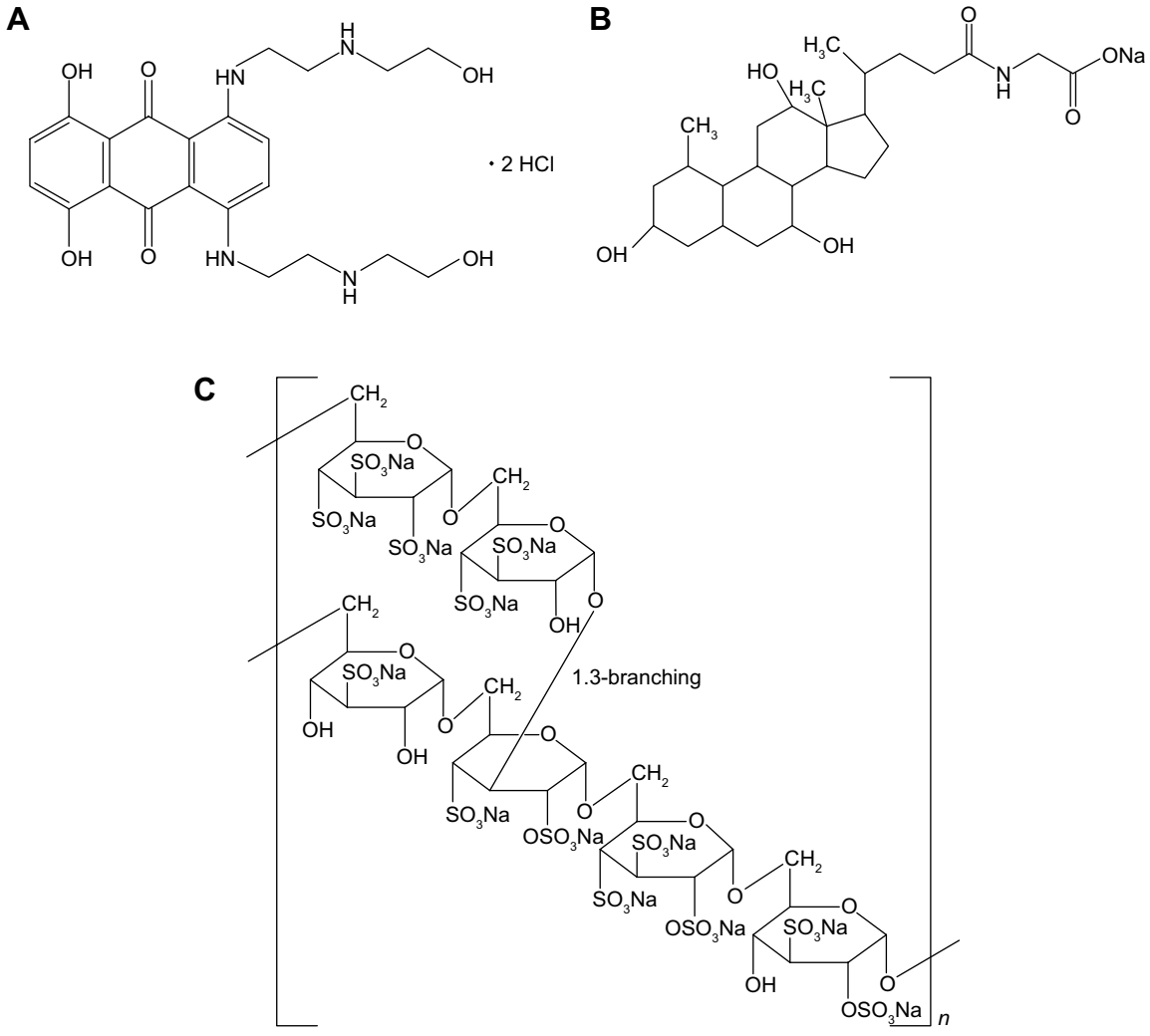


**Figure S1** Chemical structures of (**A**) mitoxantrone hydrochloride, (**B**) sodium glycocholate (GcNa), and (**C**) dextran sulfate sodium.

ethanol/0.1 M HCl (3:1, v/v) were mixed by sonication for 5 minutes to destroy the nanoparticles and then the volume was metered. After filtration by 0.45 μm filter membrane, an aliquot of suitable volume filtrate was analyzed by UV spectrophotometer for the determination of MTO. The encapsulation efficiency was calculated by the percent ratio of the amount of MTO incorporated into the nanoparticles to the initial total loading amount of MTO.

### Transmission electron microscopy

The morphology of MTO-TMLGNs was examined using TEM (H-600; Hitachi, Tokyo, Japan). A drop of nanoparticle suspension was visualized after staining with 2% (w/v) phosphotungstic acid for 30 seconds on a copper grid under TEM.

### Differential scanning calorimetry

DSC analysis was conducted using TA-60WS Thermal Analyzer (Shimadzu, Kyoto, Japan). Samples, including MTO, cyclosporine A, GcNa, blank excipients (including Compritol 888 ATO, dextran sulfate, Cremophor RH40, 1,2-Distearoyl-*sn*-glycero-3-phosphoethanolamine-*N*-[methoxy(polyethyleneglycol)-2000], and lecithin), physical mixture of MTO, cyclosporine A, GcNa, and blank excipients, and lyophilized MTO-TMLGNs, were weighed into an aluminum pan, which were then sealed with a pinhole-pierced cover. The samples were purged with dry nitrogen at a flow rate of 20 mL/min. Heating curves were recorded at a scan rate of 10°C/min from 30°C to 300°C.

### In vitro release study

The MTO release from TMLGNs was determined using dialysis bag technique in phosphate buffer saline (pH 7.4, containing 0.2% $Na_2SO_3$). An aliquot of 4 mL of nanoparticle suspensions with an MTO concentration of 0.5 mg/mL was sealed in a dialysis tube (molecular weight cutoff –14,000 Da) and immersed in 50 mL of preheated release medium. The release was conducted in an incubator shaker set at 100 rpm and 37°C. At predetermined time intervals, 4 or 1 mL (when concentration is high) of sample was withdrawn and replaced with the same amount of fresh release medium. The amount of MTO released from the nanoparticles was determined by UV spectrophotometer at 610 nm.

## Reference

1. Zhang P, Ling G, Pan X, et al. Novel nanostructured lipid-dextran sulfate hybrid carriers (NLDCs) overcome tumor multidrug resistance of mitoxantrone hydrochloride. *Nanomedicine*. 2012;8(2):185–193.